Journal of Power Sources 242 (2013) 299–304

Contents lists available at SciVerse ScienceDirect

Journal of Power Sources

journal homepage: www.elsevier.com/locate/jpowsour

Solvothermal synthesis of α-PbO from lead dioxide and its electrochemical performance as a positive electrode material

Pengran Gao [a], Yi Liu [a], Xianfu Bu [a], Meng Hu [a], Yuan Dai [a], Xiaorui Gao [b], Lixu Lei [a,*]

[a] School of Chemistry and Chemical Engineering, Southeast University, 2 Southeast University Road, Nanjing 211189, China
[b] College of Science, Hebei University of Engineering, Handan 056038, China

HIGHLIGHTS

- PbO can be prepared by a solvothermal reaction of PbO_2 within methanol.
- The prepared PbO can discharge a capacity of 165 mAh g^{-1} at 5 mA g^{-1}.
- The prepared PbO has the discharge capacity of 90 mAh g^{-1} at 200 mA g^{-1}.
- This paper shows a new way for the recycle of spent lead acid battery.

ARTICLE INFO

Article history:
Received 11 March 2013
Received in revised form
17 May 2013
Accepted 18 May 2013
Available online 1 June 2013

Keywords:
Lead monoxide
Lead dioxide
Methanol
Solvothermal reaction
Lead acid battery
Positive material

ABSTRACT

Lead acid batteries have been widely used and have dominated the global secondary battery market. It is very important to recycle the spent batteries efficiently to eliminate possible pollution and to ensure sustainable production. In this paper, we report our investigation on the solvothermal treatment of PbO_2, which is one of the model compounds for the positive active mixture, in methanol and the subsequent calcination of its product. The results show that the solvothermal treatment of PbO_2 in pure methanol at 140 °C can produce a mixture of PbO and lead oxide carbonate, which can be calcined at a temperature below 500 °C to produce α-PbO. The as-prepared PbO powders are rod-like particles of about 0.5 micrometer in diameter and several micrometers in length, which can achieve a high discharge capacity of 165 mAh g^{-1} at the discharge current density of 5 mA g^{-1}, and more than 90 mAh g^{-1} at 200 mA g^{-1} with excellent cycle stability. This study demonstrates a new way for the reuse of lead dioxide in spent lead acid batteries to produce highly active PbO.

1. Introduction

Lead acid batteries have been widely used, dominating more than 50% share of the global secondary battery market [1]. Recently, the demand for lead acid batteries has steadily increased since electric bicycles and cars have become increasingly popular [2]. In 2010, the world's annual refined lead output reached up to 9.3 million tonnes of which about 86% was consumed in the manufacture of lead acid batteries [3,4].

Without a doubt, the wide use of lead acid batteries produces spent lead acid batteries in the same amount, and the toxicity of lead vitally requires that it be efficiently recovered from spent lead acid batteries. Spent lead acid batteries consist of four parts: 11–30 wt.% electrolyte, 24–30 wt.% lead and lead alloy grid, 30–40 wt.% lead paste, and 7–10 wt.% organics. Lead paste is composed mostly of $PbSO_4$ and PbO_2, and also a little amount of PbO and lead metal. This complexity of lead paste leads to many difficulties in the subsequent process [5,6]. Commercially, lead paste is usually reduced to metallic lead through a pyrometallurgical process. Due to the use of high temperatures (around 1000 °C), the traditional pyrometallurgical process is energy-exhaustive, and generates SO_2 gas and lead dust without desulfurization, especially in some underdeveloped areas. Thus, more and more attention is paid to a green recycling process for spent lead acid batteries, such as hydrometallurgical routes [7,8].

However, one question arises: why should we obtain lead metal rather than prepare PbO from the lead paste of spent lead acid batteries, as the lead has still to be oxidized to make PbO, exhausting more energy?

In 2009, the R.V. Kumar et al. at the University of Cambridge made one of the first attempts to produce lead oxide, which was

* Corresponding author. Tel.: +86 2552090620; fax: +86 2552090618.
E-mail address: lixu.lei@seu.edu.cn (L. Lei).

0378-7753/$ – see front matter © 2013 Elsevier B.V. All rights reserved.
http://dx.doi.org/10.1016/j.jpowsour.2013.05.077

supposed to be used as the active materials for lead acid batteries [9–11]. They reported that $PbSO_4$, PbO_2 and PbO could be treated with an aqueous solution of citric acid to generate lead citrate, which can be calcined to produce a fine PbO powder. It is a pity that the authors did not report any electrochemical property of their fine PbO powders.

At about the same time, we proposed a novel method to produce new secondary batteries from spent ones based on fully separated positive and negative active materials, from which subsequent chemical treatments were employed to produce new active materials [12–14]. As for the lead acid batteries, this method requires firstly the separation of positive plates from negative plates, which are then respectively treated to get only positive active material powders and negative active material powders, apart from their respective grid alloys. Secondly, both the positive and the negative active materials are chemically treated respectively to produce PbO for new batteries. It is known that the positive powders contain PbO_2 and $PbSO_4$, while the negative ones contain Pb, $PbSO_4$ and some additives. Consequently, to produce Pb(II) compounds, PbO_2 in the positive materials must be reduced, while Pb in the negative materials must be oxidized. The Pb(II) compounds formed during those reduction or oxidation processes are carbonated together with the $PbSO_4$ in the original mixture to form $PbCO_3$, which is then calcined to obtain fine powders of PbO for the positive and negative electrodes respectively.

In the current lead acid battery industry, leady oxide is required for both negative and positive electrodes, which is then respectively converted to porous Pb and PbO_2 during the formation. There are two dominant techniques to produce leady oxide, which are the ball-mill and the Barton-pot methods [15]. The utilization of those leady oxides is usually very low, which makes the specific energy density of lead acid batteries only 30–40 Wh kg^{-1}. Therefore, it would be of interest to synthesize PbO to obtain a higher utilization and a longer cycle-life. For example, Wang et al. [16] prepared nanocrystalline α-PbO from calcination of $PbCO_3$ and used it as the positive electrode active material. The results showed that the α-PbO discharged a capacity which was 30% higher than that of the conventional ball-milled leady oxide. Cruz et al. [17] prepared a thin α-PbO film through chemical spray pyrolysis of an aqueous solution of $Pb(CH_3COO)_2 \cdot 3H_2O$ on a lead substrate. When the film on the substrate was used as a positive plate, it maintained a discharge capacity of 100 mAh g^{-1} upon extended cycling. Karami et al. [18,19] synthesized a uniform nano-structured lead oxide via a sonochemical method, which discharged a large capacity of 140 mAh g^{-1} and even 230 mAh g^{-1} as the cathode or anode of a lead acid battery. Salavati-Niasari et al. [20] also reported that the nano-size lead oxide powder with an average particle size of 35 nm could be prepared by decomposing lead oxalate at 500 °C, but no electrochemical results are reported. Therefore, it seems that nanoparticles of PbO may be more active in lead acid batteries.

In this paper, we will demonstrate the reduction of lead dioxide by solvothermal reactions in methanol. The products will be then calcined at relatively low temperatures to produce α-PbO, which is then tested as the positive electrode materials.

2. Experimental

2.1. Material preparation

The solvothermal reactions were carried out as follows: 20 mL of methanol (99.5%, Sinopharm Chemical Reagent Co., Ltd.) and 2.00 g of lead dioxide (99.7%, Aladdin Chemical Reagent Co., Ltd.) were added to a Teflon-lined stainless steel autoclave, which was heated at a temperature under stirring for a period of time. The yellow or orange solid obtained was filtered and dried.

For the investigation of the best reaction temperature, the reactions were carried out for 24 h at 60, 80, 100, 120, 140 and 160 °C respectively; for that of the best reaction time, they were carried out at 140 °C for 3, 6, 12, 18, 24 and 48 h respectively.

To prepare samples for the electrochemical studies, the solvothermal reaction was carried out at 140 °C for 24 h. The obtained solid was then calcined at 300, 350, 400, 450 °C for 1 h, respectively. The samples are sequentially denoted as A, B, C and D.

2.2. Characterization

Powder X-ray diffraction (XRD) patterns of the samples were measured on a Bruker D8 Discover instrument operating at 40 kV and 20 mA, by using CuKα radiation ($\lambda = 0.15406$ nm). The phase compositions were determined by the software Jade. Scanning electron micrographs (SEM) of samples were taken on a Hitachi S-4800 microscope. The thermogravimetric analysis (TG) of the precursor was conducted on a TA Instruments SDT-Q600 in static air with a rate of 10 °C min^{-1}.

2.3. Electrode preparation

1.0 g of the as-prepared sample (A, B, C, or D) was placed in a container, and then 0.003 g of fibres, 0.003 g of graphite, 0.124 mL of water and 0.11 mL of H_2SO_4 (36 wt.%) were added to it slowly. The amount of water added could be slightly modified to obtain the required density (4.0 g mL^{-1}). The plates were obtained by applying the paste evenly onto a Pb–Ca alloy grid with dimensions of $10 \times 8 \times 2$ mm^3.

The plates were then immersed in sulfuric acid of 8 wt.% for 5 s. After that, they were put into an oven, maintaining at a temperature of 100 °C for 5 min, and then put in a water bath, lowering the temperature to 75 °C with relative humidity >95%. The curing was conducted for 24 h. After that, the plates were dried at 70 °C for 48 h. The mass of the active material was the mass of the dried plate minus that of the blank grid.

2.4. Electrochemical performance test

All the formation and the cycling tests were carried out with an NEWARE Cycler (BTS-5V3A Shenzhen NEWARE Electronics Co., Ltd., China). The positive plate was assembled with a commercial negative plate (the area is about 3 times the size of the positive plate) and separated by absorptive glass-mat (AGM). The electrodes were assembled into a case and the electrolyte was a H_2SO_4 solution with a relative density of 1.23 g mL^{-1}.

After the plate had been soaked for 2 h, the battery formation was started. The formation was divided into 3 steps. Firstly, the electrode was charged at a current density of 15 mA cm^{-2} to 100 mAh g^{-1}; then it was charged at 25 mA cm^{-2} for another 150 mAh g^{-1}; and finally, it was charged at 8 mA cm^{-2} for another 100 mAh g^{-1}. Since the negative electrode had a much larger capacity than the positive electrode, the cell capacity was restricted by the positive electrode.

After formation, the cell was discharged at 5 mA g^{-1} until the voltage fell to 1.75 V. Then it was used for cycling tests. The electrode was first charged at 50 mA g^{-1} until the cell voltage reached 2.45 V, then it was charged at 25 mA g^{-1} until 110% of the first discharge capacity after formation was charged. The electrode was then discharged at a current density of 50 mA g^{-1}. This was done for 50 cycles.

The cyclic voltammetry (CV) was carried out on the CorrTest model CS350 electrochemical working station (WUHAN CORRTEST Instrument Co., Ltd., China). The CV curves were determined with a typical three-electrode system. The working electrode was the as-

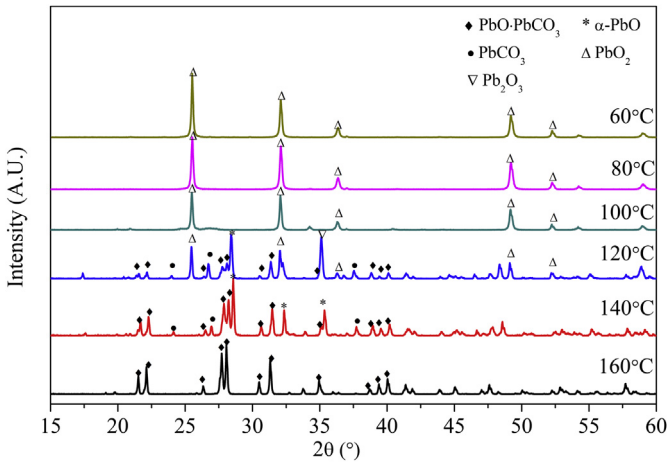

Fig. 1. XRD patterns of solvothermal products at different reaction temperatures for 24 h. The phases are identified according to the JCPDS files: $PbO{\cdot}PbCO_3$ (48-1888), α-PbO (72-151), $PbCO_3$ (52-1527), PbO_2 (89-2805) and Pb_2O_3 (2-539).

prepared electrode, and a double platinum electrode was used as the counter electrode while the $Hg/Hg_2SO_4/K_2SO_4$ (sat.) was employed as the reference electrode. Sulfuric acid (36 wt.%) was used as electrolyte. The measurement was carried out at a potential scan rate of 10 mV s^{-1} from 0 to 1.7 V.

3. Results and discussion

3.1. The solvothermal reaction of lead dioxide in methanol

It is known that PbO_2 is a strong oxidant; therefore we have tried to use CH_3OH as the reductant. Experiments carried out at temperatures below the boiling point of methanol failed, therefore, we tried to let them react at higher temperatures in a closed vessel. The following is what we found.

Fig. 1 shows the XRD patterns of the solvothermal products at different reaction temperatures. It has been found that lead dioxide does not basically react with methanol under 100 °C. As the temperature is elevated to 120 °C, both α-PbO and $PbO{\cdot}PbCO_3$ are formed, but PbO_2 still remains. At 140 °C, PbO_2 can no longer be identified, and both α-PbO and $PbO{\cdot}PbCO_3$ are found in the products. At 160 °C, $PbO{\cdot}PbCO_3$ is the only product identified. As this

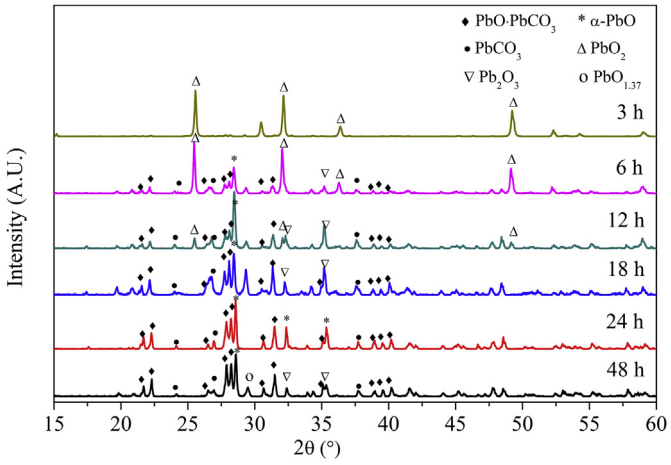

Fig. 2. XRD patterns of solvothermal products produced at 140 °C at different time. The phases are identified according to the JCPDS files: $PbO{\cdot}PbCO_3$ (48-1888), α-PbO (72-151), $PbCO_3$ (52-1527), β-PbO_2 (89-2805), Pb_2O_3 (2-539) and $PbO_{1.37}$ (27-1202).

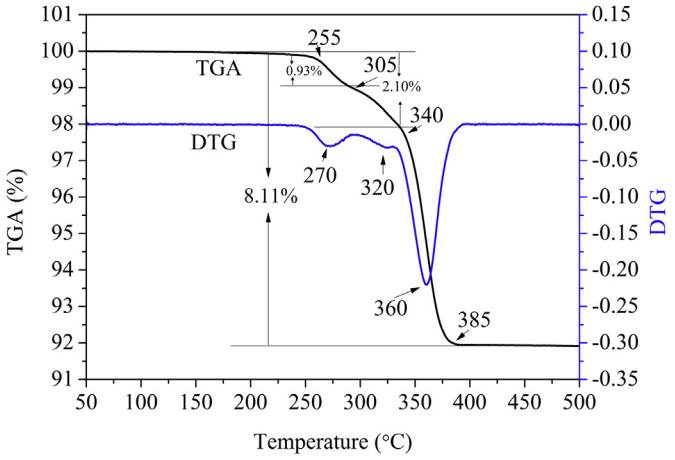

Fig. 3. TG–DTG curves of precursor after reacted at 140 °C for 24 h.

research is to prepare α-PbO, we have further studied reactions at 140 °C, without using other temperatures to eliminate energy consumption.

Fig. 2 shows the XRD patterns of the solvothermal products produced at 140 °C for different time. It is found that α-PbO and $PbO{\cdot}PbCO_3$ are identified after 6 h, but PbO_2 disappears only after 18 h. It could be noticed that α-PbO occupies a bigger fraction than $PbO{\cdot}PbCO_3$, but after 24 h, the composition seems to stabilize, and the products are getting crystallized better. This may mean that the solvothermal reaction of lead dioxide and methanol may firstly produce PbO, and then PbO reacted with CO_2 from the full-oxidation of methanol to form $PbO{\cdot}PbCO_3$:

$$3PbO_2 + CH_3OH \rightarrow 3PbO + CO_2 + 2H_2O \quad (1)$$

$$PbO + CO_2 \rightarrow PbCO_3 \quad (2)$$

$$2PbO + CO_2 \rightarrow PbO{\cdot}PbCO_3 \quad (3)$$

Therefore, the final product is a mixture of PbO and $PbO{\cdot}PbCO_3$ as the molar ratio of PbO and CO_2 in product is 3 to 1 (reaction

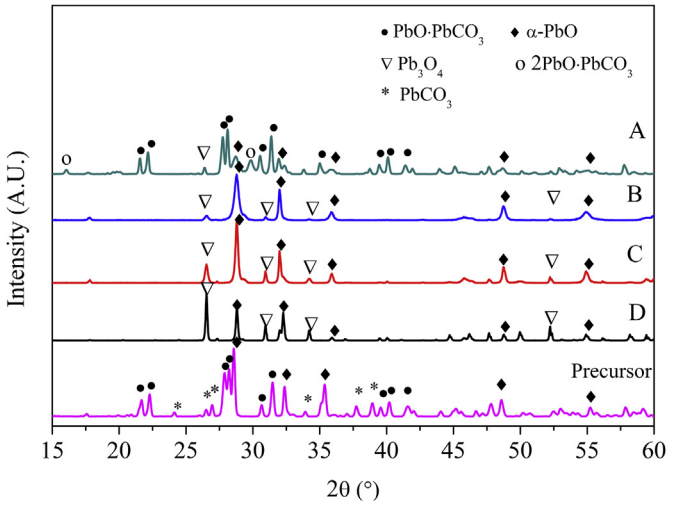

Fig. 4. XRD patterns of samples A, B, C, D, which were prepared from the calcination of the precursor at 300 °C, 350 °C, 400 °C and 450 °C for one hour, respectively. The phases are identified according to the JCPDS files: $PbO{\cdot}PbCO_3$ (48-1888), α-PbO (72-151), Pb_3O_4 (73-532), $2PbO{\cdot}PbCO_3$ (17-731) and $PbCO_3$ (52-1527).

Table 1
The composition of the samples B, C and D.

Sample	Composition (wt.%)[a]	
	PbO	Pb_3O_4
B	90.7	9.3
C	86.1	13.9
D	73.4	26.6

[a] The compositions were determined according to the XRD patterns shown in Fig. 4 with the software Jade.

(1)). Because the well-crystallized sample may not be suitable for the fine powder of PbO, so we decide to carry out the reaction at 140 °C for 24 h, and the product will be marked as precursor hereafter.

3.2. The preparation of the samples and their formation in positive electrode of a lead acid battery

PbO must be obtained for the electrochemical investigations. Therefore, we investigated the pyrolysis of the precursor. Fig. 3 shows the TG–DTG curves in static air of the precursor obtained from the solvothermal reaction between PbO_2 and methanol at 140 °C for 24 h. As it is shown, there are three losses of mass at around 270, 320 and 360 °C. Fig. 4 shows the XRD patterns of the products after the precursor being calcined at 300, 350, 400 and 450 °C for one hour respectively. It can be noticed that there are $PbO \cdot PbCO_3$, $2PbO \cdot PbCO_3$ and PbO in the sample obtained at 300 °C, but there are mainly PbO and Pb_3O_4 in the samples obtained at the temperatures higher than 350 °C; also, the amount of Pb_3O_4 increases as the temperature goes up (Table 1).

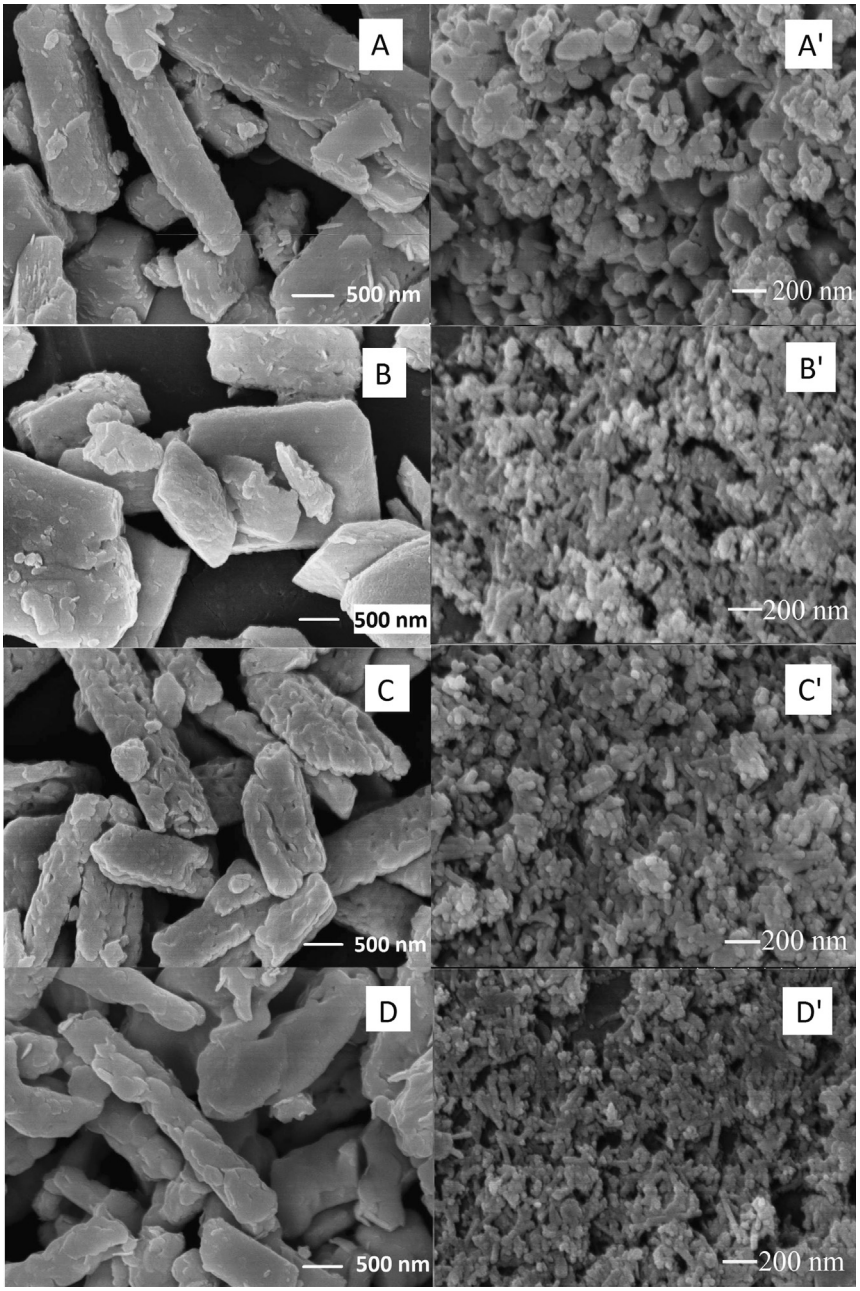

Fig. 5. SEM micrographs of the samples before (A, B, C, D) and after (A′, B′, C′, D′) formation at temperatures of (A, A′) 300 °C, (B, B′) 350 °C, (C, C′) 400 °C, (D, D′) 450 °C.

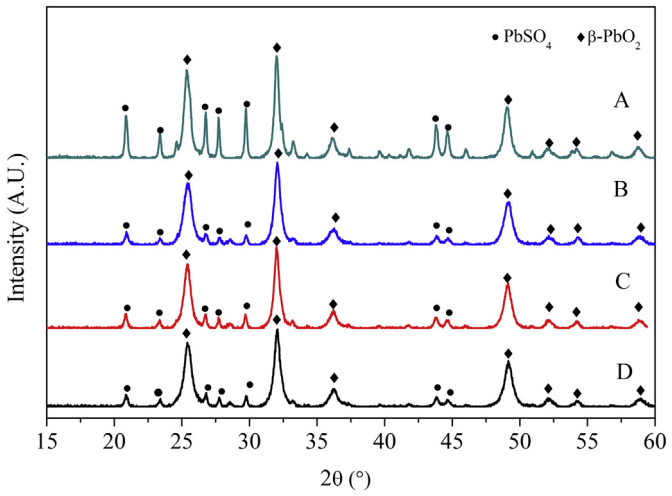

Fig. 6. XRD patterns of the four samples after formation. They are indexed according to JCPDS files: β-PbO_2 (89-2805) and $PbSO_4$ (5-577).

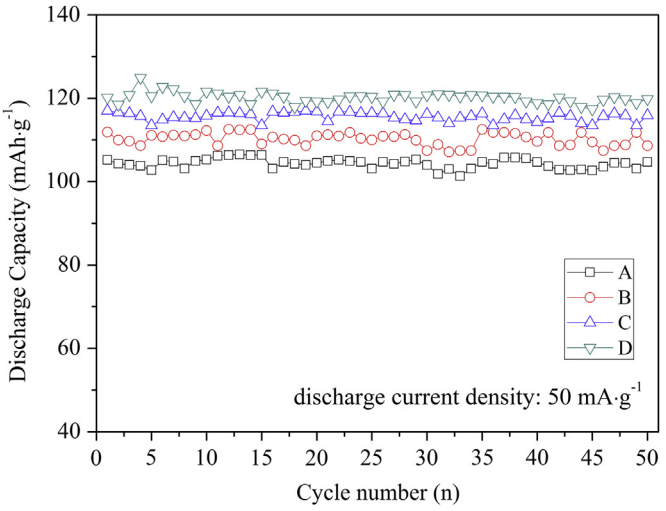

Fig. 7. The discharge capacity of the four samples at different calcination temperatures versus cycle number.

It has been known that $PbCO_3$ decomposes in three steps between 180 and 350 °C (reactions (4)–(6)) [21], and the precursor is a mixture of $PbO{\cdot}PbCO_3$, α-PbO and $PbCO_3$. Combined with Fig. 4, it can be concluded that reactions (4) and (5) are the main reactions in the range of 255–340 °C, and after that, reactions (6) and (7) become dominant. It is known that PbO can be oxidized in air, and it can certainly be accelerated at higher temperatures:

$$2PbCO_3 \rightarrow PbO{\cdot}PbCO_3 + PbO + CO_2 \quad (4)$$

$$2PbO{\cdot}PbCO_3 \rightarrow 2PbO{\cdot}PbCO_3 + PbO + CO_2 \quad (5)$$

$$2PbO{\cdot}PbCO_3 \rightarrow 3PbO + CO_2 \quad (6)$$

$$PbO + O_2 \rightarrow Pb_3O_4 \quad (7)$$

Fig. 5 shows the SEM images of the four samples, together with that of the samples after the electrode formation. It shows that samples calcined at 300, 400 and 450 °C are rod-like particles with dimensions of 0.5 μm in diameter and 2–3 μm in length. However, the sample calcined at 350 °C looks like micro-flakes. This may be related to that the decomposition of $PbCO_3$ reaches its highest rate (Fig. 3), which may enable the growth of the crystals. However, when the temperatures are either below or above 350 °C, it is possible that the diffusion required by growth of crystals is either too slow in speed or too short in time, which makes the morphology inherit that of the precursor.

To observe the morphology changes of the sample after formation, the active materials were peeled from the electrode after formation, and then grinded for SEM observations. It can be seen that the particles become much smaller after formation, but the heritage of morphology of the precursor is clear. This is because the cure process and the formation makes PbO transform into $PbSO_4$, then PbO_2 and there are substantial changes in chemical structures.

Table 2
The contents of PbO_2 after formation determined by the software Jade.

Temperature of calcination of the precursor (°C)	Contents of β-PbO_2 (wt.%)
300	88.7
350	93.8
400	94.4
450	94.6

According to the XRD patterns of the samples after formation in Fig. 6, all the four samples contain both β-PbO_2 and $PbSO_4$. According to the software Jade, the content of PbO_2 increases as the calcination temperature increases (Table 2), and the amount of $PbSO_4$ in sample A is much higher than that in the others. Combined with Table 1 and Fig. 4, it could be concluded that a higher amount of existence of Pb_3O_4 may enhance the formation. This is in accordance with the general knowledge on this particulate issue [22–24].

3.3. Electrochemical performance of the prepared samples

Fig. 7 shows the cyclic performance of the four samples, in which the discharge current density was 50 mA g^{-1}. It can be seen that the capacity of the four samples is quite stable within the 50 cycles, and the discharge capacity for the sample prepared at 300 °C is about 105 mAh g^{-1}, and the others obtained at 350, 400 and 450 °C are about 110, 116 and 120 mAh g^{-1}, respectively. The values of discharge capacities are paralleled to the content of Pb_3O_4 in the samples as well as that of β-PbO_2 in the samples after formation.

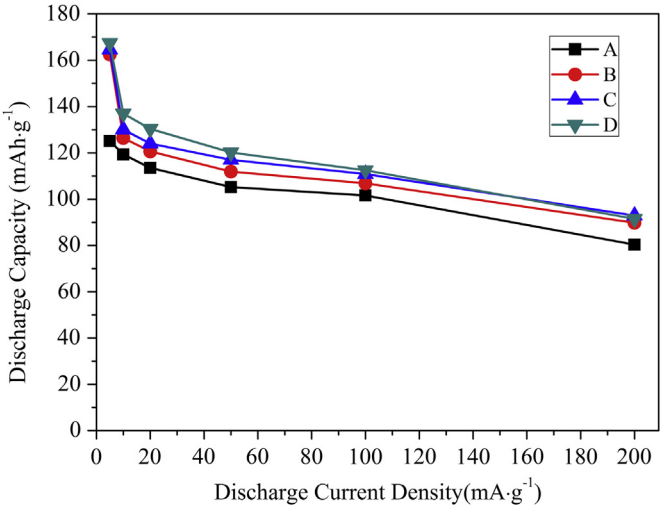

Fig. 8. Discharge capacity versus the current density of the four samples.

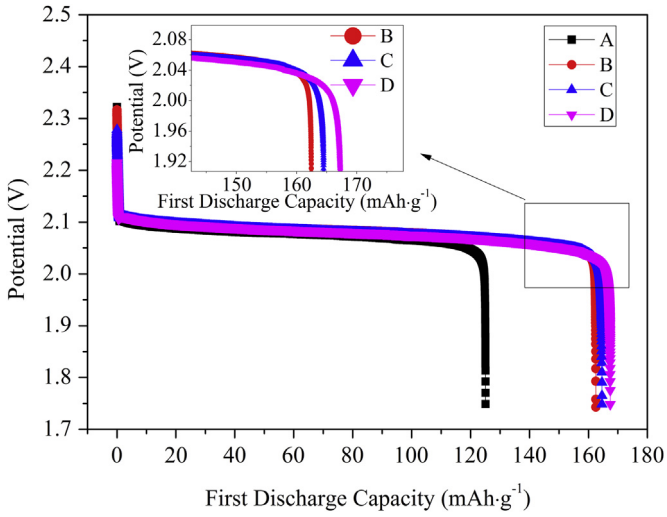

Fig. 9. The curves of potential versus first discharge capacity of the four samples.

Fig. 8 shows the curves of discharge capacity versus the current density. As expected, the discharge capacity decreases as the current density increases, the other samples discharge more than 90 mAh g^{-1} at the current density of 200 mA g^{-1}, except sample A.

Fig. 9 gives the first discharge curves of potential versus capacity at a current density of 5 mA g^{-1}. As evidence in that, the first discharge capacity of the sample A is about 125 mAh g^{-1}, while those of the other three samples are more than 160 mAh g^{-1}. Here, the utilization of active material is defined as the ratio of the discharge capacity and the corresponding theoretical capacity of PbO. The theoretical capacity of pure PbO is 240 mAh g^{-1}. The utilizations of the four samples are about 52, 67, 68 and 70%, respectively. To best of our knowledge, that is the second highest discharge capacity in lead acid batteries if lead monoxide is used in the first place as the positive electrode material.

The calcined products are also examined by cyclic voltammetry, which give the similar results to those of Visscher [25]. Fig. 10 shows the CV curves of the four samples after the 25th cycle. It can be seen that the oxidation of $PbSO_4$ to PbO_2 occurs at 1.25 V (vs. Hg/Hg_2SO_4 in sat. K_2SO_4), the evolution of oxygen occurs beyond 1.4 V, and the reduction of PbO_2 to $PbSO_4$ is at 0.93 V. All the CV curves are similar, and the cathode current is much higher than the anode current.

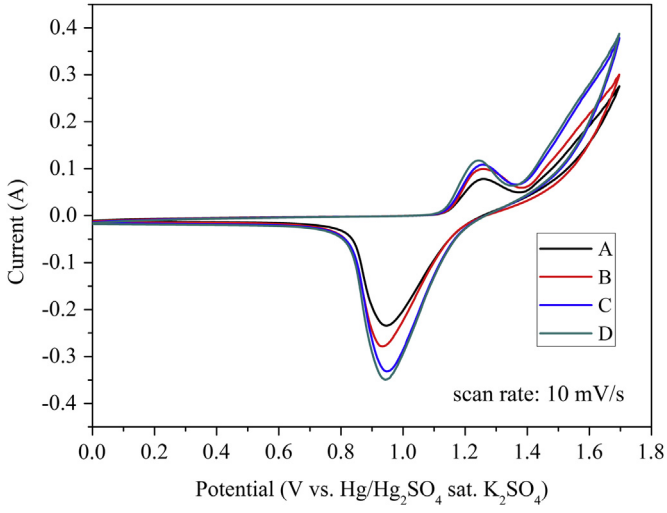

Fig. 10. Cyclic voltammetry curves of the four samples.

4. Conclusion

The PbO_2 can be reduced to α-PbO in methanol in a closed vessel at 140 °C for 24 h, and some of the methanol is fully oxidized to form CO_2. The resulted material (the precursor) is a mixture of PbO, $PbO \cdot PbCO_3$ and $PbCO_3$, because the CO_2 reacts with α-PbO to produce $PbO \cdot PbCO_3$ and $PbCO_3$.

Calcination of the precursor at 300 °C produces a mixture of α-PbO, $PbO \cdot PbCO_3$, $2PbO \cdot PbCO_3$, and small amount of Pb_3O_4; calcination of the precursor at 350, 400 or 450 °C can eliminate the carbonates. That is, only α-PbO and Pb_3O_4 are observed in the mixture. Moreover, the amount of the Pb_3O_4 increases with the temperature. Except for the sample calcined at 350 °C, which is flake-like in morphology, all the others are rod-like. After formation, those particles become much smaller, but still in similar.

The results of the electrochemical performance of the four samples show that the sample obtained at 450 °C has the largest discharges capacity, which is 165 mAh g^{-1} at 5 mA g^{-1}, and 90 mAh g^{-1} at 200 mA g^{-1}; and the sample obtained at 300 °C is the worst, which is 125 mAh g^{-1} at 5 mA g^{-1}, and 80 mAh g^{-1} at 200 mA g^{-1}. The discharge capacities of samples obtained at 350 and 400 °C are more than 160 mAh g^{-1} at 5 mA g^{-1}, and around 90 mAh g^{-1} at 200 mA g^{-1}. All the four samples behave excellently in terms of cyclic stability, their capacity loss are less than 1% in 50 cycles when they are fully discharged at 50 mA g^{-1}.

Acknowledgments

The authors would like to thank China Huafu Holding Group, the Department of Education for the Fundamental Research Funds for the Central Universities, Jiangsu Province for the College graduate research and innovation projects (CXLX12_0105), Analytical test Fund of Southeast University (201226), and Hebei Provincial Natural Science Foundation of China (B2012402006) for the financial support.

Reference

[1] M.A. Kreusch, M.J.J.S. Ponte, H.A. Ponte, N.M.S. Kaminari, C.E.B. Marino, V. Mymrin, Resour. Conserv. Recy. 52 (2007) 368–380.
[2] H.Y. Chen, A.J. Li, D.E. Finlow, J. Power Sources 191 (2009) 22–27.
[3] T.W. Ellis, A.H. Mirza, J. Power Sources 195 (2010) 4525–4529.
[4] A.M. Genaidy, R. Sequeira, T. Tolaymat, J. Kohler, M. Rinder, Sci. Total. Environ. 407 (2008) 7–22.
[5] L.C. Ferracin, A.E. Chacon-Sanhueza, R.A. Davoglio, L.O. Rocha, D.J. Caffeu, A.R. Fontanetti, R.C. Rocha, S.R. Biaggio, N. Bocchi, Hydrometallurgy 65 (2002) 137–144.
[6] T.T. Chen, J.E. Dutrizac, Hydrometallurgy 40 (1996) 223–245.
[7] Z. Vaysgant, A. Morachevsky, A. Demidov, E. Klebanov, J. Power Sources 53 (1995) 303–306.
[8] M.A. Rabah, M.A. Barakat, Renew. Energ. 23 (2001) 561–577.
[9] M.S. Sonmez, R.V. Kumar, Hydrometallurgy 95 (2009) 53–60.
[10] X.F. Zhu, L. Li, X.J. Sun, D.N. Yang, L.X. Gao, J.W. Liu, R.V. Kumar, J.K. Yang, Hydrometallurgy 117 (2012) 24–31.
[11] L. Li, X. Zhu, D. Yang, L. Gao, J. Liu, R.V. Kumar, J. Yang, J. Hazard. Mater. 203–204 (2012) 274–282.
[12] L. Lei, P. Gao, X. Lv, X. Yu, L. Cao, Y. Dai, Abstracts of Papers of the American Chemical Society. Anaheim, CA (Mar 27–31, 2011), p. ENVR-226.
[13] L. Lei, P. Gao, Y. Dai, CN-Patent, 102263309 (2011).
[14] L. Lei, CN-Patent, 101488597, (2009).
[15] D.A.J. Rand, J. Power Sources 28 (1989) 107–111.
[16] J. Wang, S. Zhong, G.X. Wang, D.H. Bradhurst, M. Ionescu, H.K. Liu, S.X. Dou, J. Alloys Compd. 327 (2001) 141–145.
[17] M. Cruz, L. Hernan, J. Morales, L. Sanchez, J. Power Sources 108 (2002) 35–40.
[18] H. Karami, M.A. Karimi, S. Haghdar, A. Sadeghi, R. Mir-Ghaserm, S. Mahdi-Khani, Mater. Chem. Phys. 108 (2008) 337–344.
[19] H. Karami, M.A. Karimi, S. Haghdar, Mater. Res. Bull. 43 (2008) 3054–3065.
[20] M. Salavati-Niasari, F. Mohandes, F. Davar, Polyhedron 28 (2009) 2263–2267.
[21] S.A.A. Sajadi, A.A. Alamolhoda, Inorg. Mater. 42 (2006) 1099–1103.
[22] L.T. Lam, I.G. Mawston, D. Pavlov, D.A.J. Rand, J. Power Sources 48 (1994) 257–268.
[23] C.V. D'Alkaine, J. de Andrade, P.R. Impinnisi, J. Power Sources 85 (2000) 131–136.
[24] J. Wang, S. Zhong, H.K. Liu, S.X. Dou, J. Power Sources 113 (2003) 371–375.
[25] W. Visscher, J. Power Sources 1 (1977) 257–266.